ISSN 1063-7826, Semiconductors, 2017, Vol. 51, No. 5, pp. 549–555. © Pleiades Publishing, Ltd., 2017.
Original Russian Text © V.M. Korol', A.V. Zastavnoi, Yu. Kudriavtsev, R. Asomoza, 2017, published in Fizika i Tekhnika Poluprovodnikov, 2017, Vol. 51, No. 5, pp. 579–584.

NONELECTRONIC PROPERTIES OF SEMICONDUCTORS (ATOMIC STRUCTURE, DIFFUSION)

Negative Annealing in Silicon after the Implantation of High-Energy Sodium Ions

V. M. Korol'[a]*, A. V. Zastavnoi[a], Yu. Kudriavtsev[b], and R. Asomoza[b]

[a] *Southern Federal University, Institute of Physics, Rostov-on Don, 344090 Russia*

[b] *Department Ingenieria Electrica–SEES, Cinvestav-IPN, 07360 Mexico*

**e-mail: vkorol@ctsnet.ru*

Submitted November 1, 2016; accepted for publication November 14, 2016

Abstract—The implantation of sodium ions with an energy of 300 keV is carried out into high-resistivity *p*-Si. The annealing of defects at T_{ann} = 350–450°C and related activation of atoms (the latter occurs at the "tail" of atom distribution) are described by a first-order reaction. At T_{ann} = 450–525°C and irrespective of the ion dose, negative annealing is observed; this annealing is accompanied by an appreciable increase in the surface resistance ρ_s. According to estimations, the activation energy of this process amounts to ~2 eV. It is our opinion that the annealing is related to the precipitation of sodium donor atoms, which occurs at a depth exceeding by two–three times the projected range R_p of ions. The annealing of defects at T_{ann} = 525–700°C, which leads to a further decrease in ρ_s, features an activation energy of ~2.1 eV. The hypothesis that the "tail" in the profiles of sodium atoms measured by secondary-ion mass spectroscopy is due to the diffusion of these atoms from the walls of the crater to its center is verified. It is shown that this process is not implemented since the profiles of sodium atoms measured at room temperature do not differ from those measured at –140°C.

DOI: 10.1134/S1063782617050141

1. INTRODUCTION

Negative annealing is observed in the case of the implantation into silicon of traditional impurities; this annealing is characterized by a decrease in the sheet conductivity (to be more precise, a decrease in the surface concentration of electrically active atoms [1]) with an increase in the annealing temperature. This process has been studied in detail for implanted boron whose atoms transfer (under the effect of the flux of interstitial silicon atoms liberated as a result of the disintegration of "end-of range" cluster defects) from lattice sites to interstitial positions and, thus, lose their electrical activity. A similar effect was also observed in the case of implanted phosphorus [1] and, possibly, due to the same cause as in the case of boron [2]; however, there are no experiments directed at determination of the positions of phosphorous atoms. Negative annealing for the above-mentioned is observed at an implantation dose sufficient for amorphization or close to this dose.

Recently [3], in studying the isochronous annealing of silicon doped by the implantation of high-energy sodium ions (E = 300 keV, $\Phi = 5 \times 10^{14}$ and 3×10^{15} cm^{-2}), an increase in the surface resistance ρ_s is observed in the temperature range of T_{ann} = 450–550°C; however, this effect was not commented upon in [3]. It is unlikely that the effect under consideration is caused by accidental outlier of experimental points since the increase in ρ_s was observed in all studied samples (two–three samples per dose of ions). Taking into account the unusual behavior of sodium impurity in silicon [4], the purpose of this study consisted in detailed examination of the above phenomenon. According to our opinion, the nature of negative annealing is related to a loss of donor sodium atoms as a result of their interaction with interstitial silicon atoms and subsequent precipitation at depth, which exceed the projected range R_p by two–three times.

2. EXPERIMENTAL

In this study, we used a silicon ingot similar to that used in [3]; i.e., the ingot was grown by the floating-zone method (FZ-Si) along the ⟨111⟩ axis, the doping impurity was boron, and the resistivity was ρ = 2–3 kΩ cm. Sodium ions were implanted at an energy of E = 300 keV and doses of $\Phi = 6 \times 10^{13}$–3×10^{15} cm^{-2}. In order to reduce channeling, the normal to the sample surface diverged by an angle of 7° from the ion-beam axis. The samples were annealed in a quartz tube in air. The isothermal annealing (T_{ann} = 350–850°C, t_{ann} = 15 min), isochronous annealing, and profiles of the free-electron concentration $n(x)$ were studied using the four-probe method. Thin layers were removed by the method of anodic oxidation with the subsequent

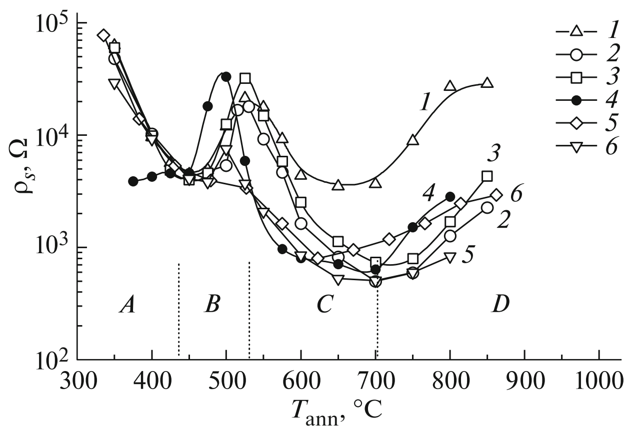

Fig. 1. Dependence of the surface resistance ρ_s on the temperature of annealing. E = (*1–4*) 300, (*5*) 200, and (*6*) 50 keV. Φ = (*1*) 6 × 10^{13}, (*2*) 5 × 10^{14}, (*3, 4*) 1 × 10^{15}, and (*5, 6*) 2 × 10^{15} cm^{-2}; and t_{ann} = (*1–3*) 15 and (*4*) 45 min.

dissolution of oxide in HF. In calculations of the profiles $n(x)$, the mobility of charge carriers was determined from its empirical dependence on the concentration of electrically active phosphorus atoms [6]; the effect of radiation-induced defects on the mobility of charge carriers was disregarded.

The profiles of sodium atoms were measured by the method of secondary-ion mass spectrometry (SIMS). We used a time-of-flight TOF-SIMS-V spectrometer (Ion-TOF GmbH Co.) in the "double beam" mode. Sputtering of the surface was performed using a beam of O_2^+ ions with an energy of 2 keV over an area of 300 × 300 μm. Secondary positive ions sputtered by a pulsed beam of 30-keV Bi^+ ions from the central part of the etching crater (with a size of 100 × 100 μm) were analyzed. The angle of incidence for both beams amounted to 45°. The depth of the crater was measured using a Dektak-XT profilometer produced by Bruker Co. The concentration profile of sodium atoms was calculated on the basis of the implantation dose.

3. EXPERIMENTAL RESULTS AND DISCUSSION

In this study, we used a smaller step in terms of temperature (15–25°C) compared to that in [3] in investigating the results of isochronous annealing; this made it possible to observe more precisely the boundaries of negative annealing (Fig. 1). An increase in the duration of annealing from 15 to 45 min (curve *4*) barely varies the shape of the dependence $\rho_s(T_{ann})$; however, it shifts the maximum of ρ_s at T_{ann} = 525°C to the left by 25°C. The temperature range of annealing in Fig. 1 is divided into four regions (*A–D*) for convenience in consideration of the occurring processes. The boundaries of these regions are somewhat arbitrary since the results of annealing depend on both the temperature and duration of annealing. At T_{ann} = 350–450°C, a decrease in ρ_s in the region *A* is conventionally related to the annealing of simple radiation-induced complexes, which compensate the conductivity of the doped layer. In the region *B* (T_{ann} = 450–525°C), a decrease in ρ_s is replaced by its appreciable increase (negative annealing). It is important to note that the characteristics of this process are practically independent of the dose of implantation. However, the energy of ions significantly affects the shape of curves $\rho_s(T_{ann})$. For example, at E = 50 keV, we observe only a narrow plateau (curve *5*) instead of a peak in ρ_s (Fig. 1, curves *1–4*); i.e., negative annealing becomes barely distinguishable. The annealing of defects in the region *C* at T_{ann} = 525–700°C leads to a decrease in ρ_s. At E = 300 keV and $\Phi > 6 \times 10^{13}$ cm^{-2}, the smallest value of ρ_s is attained at T_{ann} = 700°C, whereas this takes place at 600°C in the case of E = 50 keV. Finally, in the region *D* at T_{ann} > 700°C, ρ_s again increases (second negative annealing), the cause of which is the reverse diffusion of donor sodium atoms to the surface. Reaching the region of most damage, sodium atoms interact with defects and lose electrical activity; as T_{ann} is further increased, they evaporate with the vast majority of deactivated atoms [3, 5].

The measurements of positions occupied by implanted atoms in a silicon lattice using the method of proton channeling in combination with the nuclear reaction $Na^{23}(p, \alpha)Ne^{20}$ showed [7] that, after annealing at 540°C for 30 min, the vast majority (87%) of these atoms are located at tetrahedral or irregular interstitial sites. However, only a small part of them (~1%) exhibits electrical activity [3–5].

We now consider the results obtained by studying the profiles of free electrons $n(x)$ (Fig. 2). The specific feature of these results obtained at T_{ann} = 450°C consists in the fact that sodium donors, irrespective of the dose, are localized at considerable depths in the range of (two–three)R_p (the parameters of the range of sodium ions at E = 300 keV, as determined using the SRIM-2013 software package [8], are R_p = 582 nm and ΔR_p = 136 nm). The same donors are responsible for relatively small values of ρ_s at T_{ann} = 350–400°C (Fig. 1). As T_{ann} is increased, the depth of the localization of sodium atoms decreases and, in addition, depends on the dose. For example, at T_{ann} = 550°C (Fig. 2b), the $n(x)$ profiles are localized at low doses at a depth of < R_p (Fig. 2b, curves *1*, *2*), while, at higher doses, i.e., $\Phi \geq 5 \times 10^{14}$ cm^{-2} (curves *3* and *4*), the profile is situated at a depth of $\geq 1.5R_p$. The fairly large variation in the depth of impurity activation with dose (Fig. 2b, curves *2* and *3*) is undoubtedly related to a

change in the defect structure of the implantation-affected layer. At T_{ann} = 600°C, we also observe a dose-related difference between the peak in the $n(x)$ profile with respect to R_p (Fig. 2c). In addition, at T_{ann} = 600°C, the intense diffusion of sodium donors located both on the left (curves *1*, *2*) and right slope of the implantation profile (curve *3*) occurs. For example, after annealing for 30 min, the depth of location of the n–p junction is as large as 35–40 μm [5]. It is worth noting that, in constructing the profiles, the effect of radiation-induced defects on the mobility of charge carriers was disregarded, the concentration of electrons in the $n(x)$ profiles is bound to be several times higher than it is shown in Fig. 2.

Free electrons recorded at $T_{ann} \leq 450$°C at a depth of (two–three) R_p are lacking here at $T_{ann} \geq 550$°C. As is known, it is exactly at these depths that the “end-of-range” defects are observed after annealing; these defects are represented by complexes of interstitial silicon atoms [9], which are visualized via the deposition of rapidly diffusing atoms of metals, for example, Cu [10]. It can be presumed that, similarly to boron atoms, which form complexes with interstitial silicon atoms [9], in the case under consideration, such complexes are formed with sodium atoms; the latter act as centers of precipitation. Kalinin et al. [11] were the first to note the presence of precipitates in silicon implanted with sodium (50 keV, 5 × 10^{14} cm^{-2}, T_{ann} = 540°C, t_{ann} = 30 min) on the basis of results obtained using transmission electron microscopy (for details, see [4]). It is also known that precipitation is observed in Fz-Si samples saturated with lithium by diffusion and irradiated with fast neutrons [12]. Due to the high mobility of lithium, its precipitation takes place even at room temperature and is accompanied by an increase in the resistivity ρ. This process features the highest rate at T_{ann} = 50°C. In another experiment, the highest rate of precipitation was observed at T_{ann} = 130°C in the Fz-Si samples saturated with lithium and without subsequent irradiation with neutrons [13]. According to the authors [13], the centers of precipitation are complexes of lithium with background impurities of carbon and oxygen. We estimated the diffusion coefficients of lithium and sodium implanted into the same silicon. We obtained the following values: $D_{Na} = 8 \times 10^{-11}$ cm^2/s at $T_{ann} \approx 480$°C and $D_{Li} = 2 \times 10^{-11}$ cm^2/s at T_{ann} = 130°C. If we take into account that D_{Na} decreases in the presence of radiation-induced defects, the diffusion coefficients for both impurities will have almost the same values at the specified temperatures.

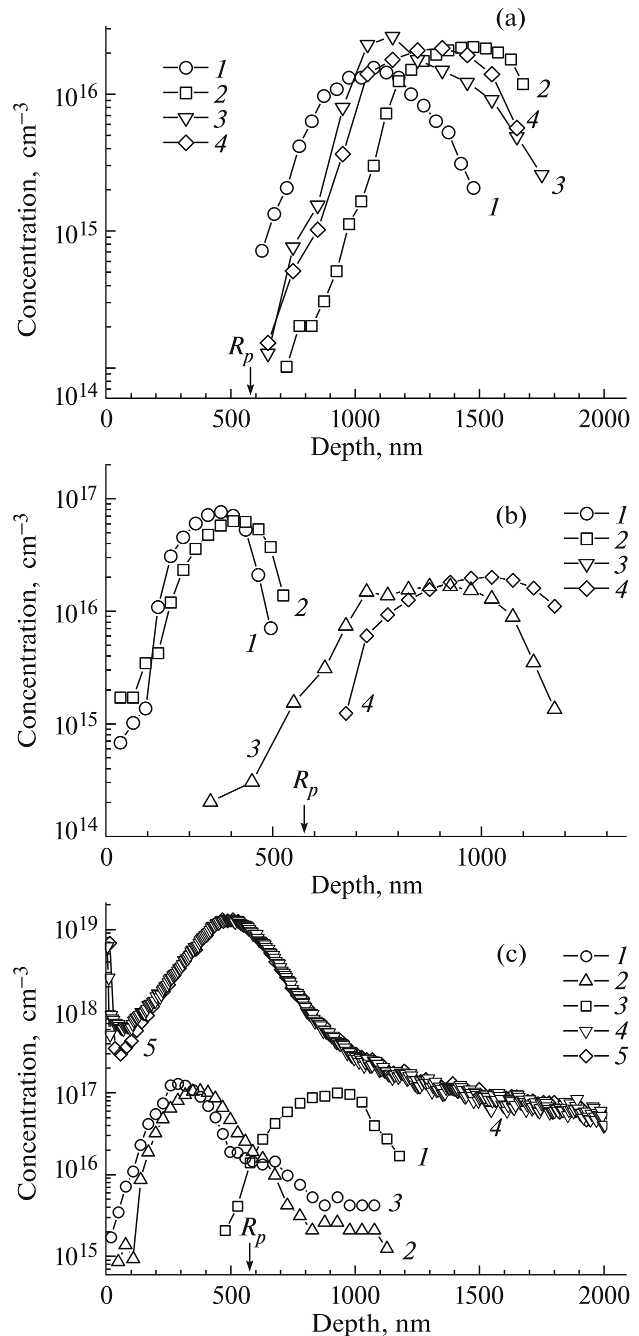

Fig. 2. Profiles of free electrons $n(x)$ at T_{ann} = (a) 450°C, (b) 550°C, and (c) 600°C. E = 300 keV, t_{ann} = 30 min; Φ = (at a, b) (*1*) 6 × 10^{13}, (*2*) 3 × 10^{14}, (*3*) 5 × 10^{14}, and (*4*) 1 × 10^{15} cm^{-2}; Φ = (at c) (*1*) 6 × 10^{13}, (*2*) 3 × 10^{14}, and (*3*) 5 × 10^{14} cm^{-2}. Figure 2c shows the profiles of sodium atoms (E = 300 keV, Φ = 5 × 10^{14} cm^{-2}, T_{ann} = 600°C, t_{ann} = 30 min) measured by the SIMS method at (*4*) at room temperature and (*5*) –140°C.

Figure 2c also shows the SIMS profile of implanted sodium (300 keV, 5 × 10^{14} cm^{-2}) after annealing at 600°C for 30 min (curve *4*). This profile completely coincides with that of sodium as measured before annealing (not shown in Fig. 2c). Both profiles include an intense “tail”, which is typically observed in the case of sodium implantation into silicon [3–5].

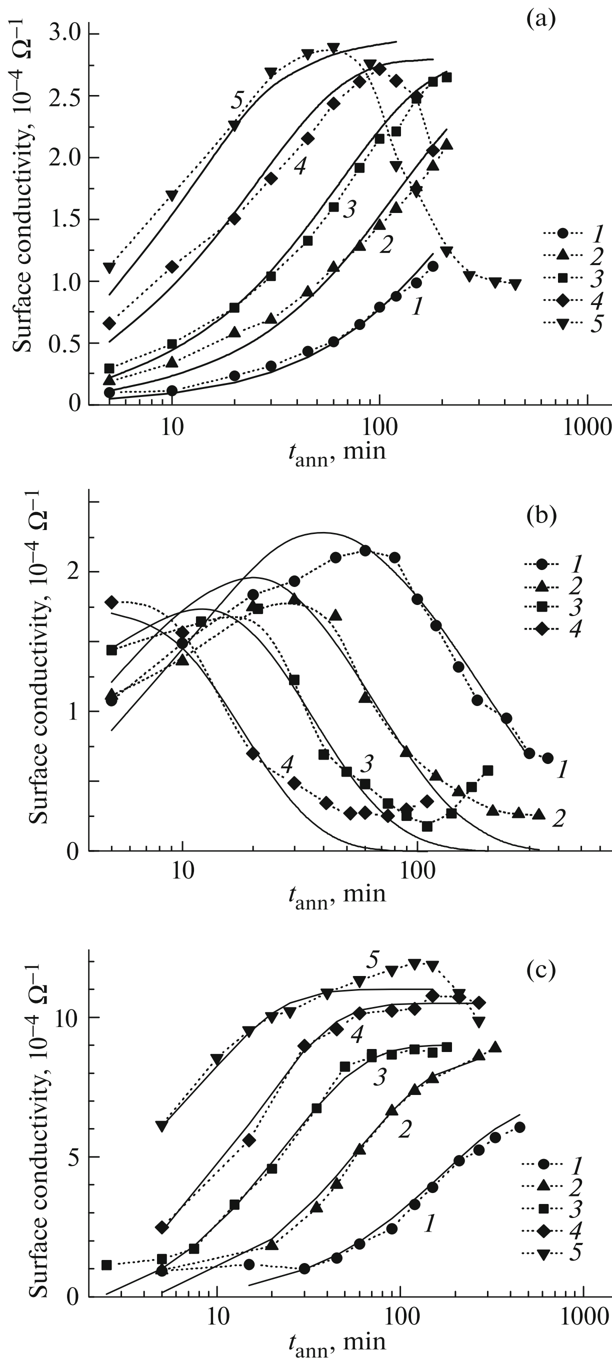

Fig. 3. Dependence of the surface conductivity σ_s on the time of annealing. T_{ann} = (in Fig. 3a) (*1*) 350°C, (*2*) 370°C, (*3*) 390°C, (*4*) 420°C, and (*5*) 435°C; in Fig. 3b: T_{ann} = (*1*) 440°C, (*2*) 460°C, (*3*) 480°C, and (*4*) 500°C; and in Fig. 3c: T_{ann} = (*1*) 545°C, (*2*) 570°C, (*3*) 600°C, (*4*) 615°C, and (*5*) 630°C. Solid lines represent the calculated dependences.

The formation of this "tail" is not related to the channeling of ions since, before implantation, we misoriented the crystallographic axis with respect to the ion-beam axis. As was mentioned above, the "tail" is caused by sodium atoms, which happen to be involved in the channeling mode after scattering at silicon atoms. Another cause of the appearance of the "tail" in SIMS measurements can be related to the diffusion of sodium atoms from crater's wells to its center during the course of measurements. In order to verify this hypothesis, we measured the sodium profile at a temperature of −140°C (Fig. 2c, curve *5*) using a standard holder made by Ion-TOF GmbH. The sample was preliminarily cleaned in an ultrasound alcohol bath, after that it was treated for 5 min in hydrochloric acid, and was finally washed in deionized water. It can be seen that both profiles do not appreciably differ from each other, except for a narrow near-surface portion related apparently to cleaning of the sample surface. Thus, it is shown that the above-suggested mechanism of appearance of the "tail" is not realized in measurements of the sodium profiles by the SIMS method.

We now consider the results of studying the isothermal annealing (Fig. 3). The dependences $\sigma_s(t_{ann})$ measured in the region *A* (Fig. 3a) represent the process of defect annealing and the related activation of sodium atoms. However, at T_{ann} = 420 and 435°C (Fig. 3a, curves *4* and *5*, respectively), a drop in σ_s is observed after the maximum in the $\sigma_s(T_{ann})$ curves is attained; this drop is caused by the dominance of the precipitation process, which was mentioned above. This example indicates some arbitrariness in defining the boundary of the regions shown in Fig. 1. Another such example is provided by the shape of annealing curves in region *B* (Fig. 3b). For the first 10–100 min (depending on T_{ann}), the conductivity σ_s increases as a result of the annealing of defects and a corresponding increase in the number of donor sodium atoms. However, a decrease in σ_s related to the precipitation of impurity occurs during subsequent annealing. Upon completion of the process of this decrease (its duration is shorter if T_{ann} is higher) σ_s again increases (curves *4*, *5*), which takes place due to an increase in the number of sodium atoms activated at smaller depths compared with those involved in annealing at T_{ann} = 450°C.

The activation and disappearance of sodium donors can be considered as a sequential irreversible reaction of the first order of the $X \rightarrow Y \rightarrow Z$ type. At the first stage of this reaction ($X \rightarrow Y$), the accumulation of donor atoms occurs (increases component *Y*). In the second stage ($Y \rightarrow Z$), a decrease in component *Y* takes place according to the formula [14]

$$[Y] = a\frac{k_1}{(k_2 - k_1)}[\exp(-k_1 t) - \exp(-k_2 t)], \qquad (1)$$

where a is the initial concentration of component *X* and k_1 and k_2 are the rates of the reactions $X \rightarrow Y$ and $Y \rightarrow Z$, respectively. The component *X* decreases

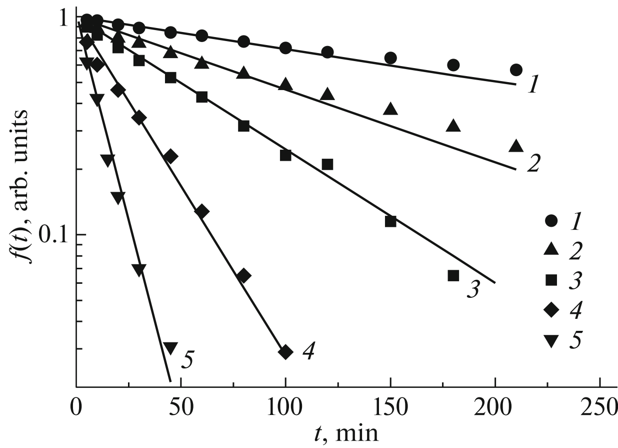

Fig. 4. Dependence of the function $f(t) = (\sigma_m - \sigma_s(t))/\sigma_m$ on the duration of annealing. T_{ann} = (*1*) 350°C, (*2*) 370°C, (*3*) 390°C, (*4*) 420°C and (*5*) 435°C.

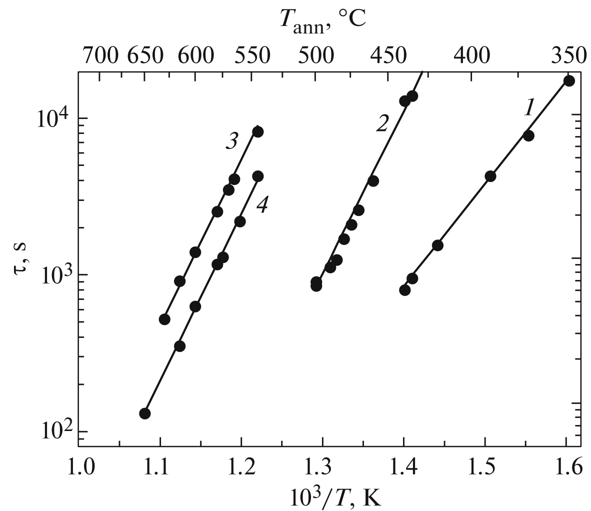

Fig. 5. Temperature dependence of the time constant τ for annealing in the regions (*1*) *A*, (*2*) *B*, and (*3*, *4*) *C*. *E* = (*1–3*) 300, (*4*) 50 keV.

steadily by exponential law with the time of annealing, whereas the component *Y* passes through a maximum at the moment of time t_m:

$$t_m = \frac{\ln r}{(r-1)k_1}, \tag{2}$$

where $r = k_2/k_1$. As applied to the case under consideration, expression (1) takes the following form after replacement $k = 1/\tau$:

$$\sigma(t) = \sigma_m \frac{\tau_2}{\tau_1 - \tau_2}\left[\exp\left(-\frac{t}{\tau_1}\right) - \exp\left(-\frac{t}{\tau_2}\right)\right]. \tag{3}$$

Here, σ_m is the largest value of the surface conductivity attainable at the first stage of annealing (this value is equal to (2.8–3) × 10^{-4} Ω^{-1}) and τ_1 and τ_2 are the characteristic times of activation and disappearance, respectively, of sodium donors as defined by the formula

$$\tau(T) = \tau_0 \exp\left(\frac{\Delta E}{kT}\right), \tag{4}$$

where *k* is the Boltzmann constant, ΔE is the activation energy of the process, and τ_0 is the preexponential factor. In some range of T_{ann} in the first stage of annealing, we can disregard the effect of the second stage, which is equivalent to the inequality $\tau_1 \ll \tau_2$. In this case, formula (1) takes the following simple form:

$$\sigma(t) = \sigma_m\left[1 - \exp\left(-\frac{t}{\tau_1}\right)\right]. \tag{5}$$

The parameters of annealing in the stage $X \rightarrow Y$ at T_{ann} = 350–435°C (Fig. 3a) were determined using an exponential approximation of the dependences plotted in relative units $f(t) = [\sigma_m - \sigma_s(t)]/\sigma_m$ (Fig. 4). Using the determined values of τ_1, we plotted the Arrhenius dependence (Fig. 5, the straight line *1*), which features the activation energy ΔE_1 = 1.3 eV and the frequency factor τ_{01} = 5.5 × 10^{-7} s. This value of ΔE_1 is typical for annealing the simplest radiation-induced defect complexes, which compensate the initial conductivity. For curves *3* and *4* (Fig. 3a), the initial increase in σ_s is followed by its decrease; the latter is related to losses of donor sodium atoms in the course of their precipitation. Nevertheless, the values of τ_1 determined for these curves are quite consistent with the linear dependence τ ($10^3/T$) (the straight line *1* in Fig. 5).

Determination of the values of τ_2 in the presence of a transient process was found to be more difficult. Due to this reason, in order to determine these values in the stage $Y \rightarrow Z$ at T_{ann} = 440–500°C, we used an indirect method, which consisted in fitting this parameter in the equation (2) so that the best agreement is attained with the experimental curves $\sigma_s(t)$. At lower T_{ann} values (the case where the role of the *Y* process is insignificant) τ_2 was estimated based on the inflection point t_m of the annealing curves $\sigma_s(t)$. The dependences $\sigma_s(t)$ calculated using the obtained values of τ_2 are shown in Fig. 3b by solid lines. These lines adequately describe the portion of growth in the curves $\sigma_s(t)$, the inflection point, the loss of sodium donors during annealing, and also a decrease in the maximum of the annealing curve as T_{ann} is increased. The obtained values of τ_2 were used to plot the temperature dependence τ ($10^3/T$) (Fig. 5, straight line *2*). It can be seen that, at T_{ann} = 435–500°C, this dependence is well reproduced by a

straight line with the parameters $\Delta E_2 = 2$ eV and $\tau_{02} = 6 \times 10^{-11}$ s. If we accept the diffusion mechanism of the precipitation process and take the value of 2 eV for the activation energy for the diffusion of sodium atoms, the obtained value of ΔE_2 is significantly larger than the energy of sodium activation in "pure" initial silicon $\Delta E = 1.28$ eV [3, 5], which can be accounted for by the effect of radiation-induced defects (the latter make sodium diffusion in the implantation layer difficult).

The Arrhenius dependence (Fig. 5, straight line *3*) in region *C* was determined by the same method as in region *A*. The corresponding parameters are $\Delta E_3 = 2.1$ eV and $\tau_{03} = 1 \times 10^{-9}$ s. Using these parameters, we obtained the calculated dependences of the annealing curves (Fig. 3c, solid lines), which fairly well reproduce experimental curves. It is worth noting that annealing in region *C* is more complicated than that in region *A*. In region *C*, each curve $\sigma_s(t_{ann})$ attains saturation (Fig. 3c), whose value increases with an increase in T_{ann}. This can indicate that there are fast and slow stages of annealing.

The straight line *4* in Fig. 5 represents the dependence $\tau(10^3/T)$ obtained using the results of measurements of the curves of isothermal annealing at $E = 50$ keV. This dependence is characterized by the same activation energy 2.1 eV as was determined in the case of $E = 300$ keV. However, the constant of its activation ($\tau_0 = 3 \times 10^{-10}$ s) in the case of $E = 50$ keV is smaller by three times than that at $E = 300$ keV; this indicates that the rate of annealing increases with a decrease in the energy of sodium ions. It is possible, thanks to the proximity of the surface, which represents a drain for mobile defects, for the pattern of negative annealing to smoothen as the ion energy is lowered.

It was mentioned above that annealing in the region *D* is accompanied by the outward diffusion of donor sodium atoms, which affects the shape of annealing curves in region *C*. This is clearly demonstrated by curve *5* in Fig. 3c; for this curve, a decrease in σ_s occurs at $t_{ann} > 200$ min.

4. CONCLUSIONS

(i) Four characteristic regions can be identified in the range of $T_{ann} = 350$–$850°C$ in the course of the isochronous annealing of high-resistivity *p*-Si doped by the implantation of high-energy sodium ions. Annealing at $T_{ann} = 350$–$450°C$, at which sodium atoms are activated, is described by a first-order reaction with the parameters $\Delta E_1 = 1.3$ eV and $\tau_{01} = 5.5 \times 10^{-7}$ s. At $T_{ann} = 450$–$525°C$, irrespective of the dose (6×10^{13}–3×10^{15} cm^{-2}), negative annealing is observed; as a result of this annealing, ρ_s increases markedly. The process is characterized by the parameters $\Delta E_2 = 2$ eV and $\tau_{02} = 6 \times 10^{-11}$ s and, in our opinion, is related to a loss of donor atoms as a result of their precipitation. It is assumed that the centers of precipitation can be complexes of sodium atoms with interstitial silicon atoms. At $T_{ann} = 525$–$700°C$, the increase in ρ_s is replaced by its decrease. The process is characterized by the parameters $\Delta E_3 \sim 2.1$ eV and $\tau_{03} = 1 \times 10^{-9}$ s. At $T_{ann} = 700$–$850°C$, ρ_s increases again, which is caused by the backward diffusion of sodium donors to the surface with subsequent evaporation.

A specific feature of the behavior for profiles of sodium donor atoms $n(x)$ is the fact that, at $T_{ann} = 450°C$, these atoms are localized at a rather large depth in the range of $(2$–$3)R_p$ irrespective of the dose. At $T_{ann} = 550°C$, the profiles at low doses are localized at a depth of $< R_p$; however, at higher doses $\Phi \geq 5 \times 10^{14}$ cm^{-2}, this occurs at the depths $\geq 1.5R_p$; i.e., the depth of localization of profiles somewhat decreases with an increase in T_{ann} as the defects are annealed. Such separation of regions of localization of profiles $n(x)$ with respect to the projected range in relation to the dose takes place also at $T_{ann} = 600°C$ when the deep (by tens of micrometers) diffusion-caused penetration of sodium atoms to the basis material is observed.

(ii) In this study, we verified the hypothesis that the appearance of a "tail" in the distribution of sodium atoms in the course of measurements by the SIMS method is due to the diffusion of these atoms from the walls of the crater to its center. To this end, we compared the sodium profiles measured at room temperature with those measured at $-140°C$. It is shown that these profiles barely differ which indicates the absence of the above-suggested mechanism of appearance of the "tail".

ACKNOWLEDGMENTS

We are grateful to V.A. Dravin who performed the implantation of high-energy ions.

This study was supported by the Ministry of Education and Science of the Russian Federation (the basis and planning parts of the State task) subject nos. 1927 (213.01-11/2014-21), 213.01-2014/012-VG, and 3.1246.2014/K.

REFERENCES

1. H. Ryssel and I. Runge, *Ion Implantation* (Wiley, Chichester, 1986; Nauka, Moscow, 1983), Chap. 3, p. 53, Chap. 6, p. 204.
2. S. Ruffer, P. J. Simpson, and I. V. Mitchll, J. Appl. Phys. **98**, 013713 (2005).

3. V. M. Korol', Yu. Kudryavtsev, A. V. Zastavnoi, and S. A. Vedenyapin, J. Surf. Invest.: X-ray, Synchrotr. Neutron Tech. **3**, 292 (2009).

4. V. M. Korol' and A. V. Zastavnoi, Poverkhnost' **5**, 74 (2001).

5. V. M. Korol', Phys. Stus Solidi A **110**, 9 (1988).

6. G. Baccarani and P. Ostojia, Solid State Electron. **18**, 579 (1975).

7. G. A. Belikov, V. M. Korol', L. K. Mamaev, and V. S. Popov, in *Proceedings of the 6th All-Union Workshop on Physics of Interaction of Charged Particles with Single Crystals* (Mosk. Gos. Univ., Moscow, 1975), p. 325.

8. J. F. Ziegler, SRIM-2013 Software Package. http://www.srim.org/.

9. C. Bonafoce, A. Claverie, D Alquier, C. Bergaud, A. Martinez, L. Laânab, and D. Mathiot, Appl. Phys. Lett. **71**, 365 (1997).

10. Y. M. Gueorgiev, R. Kögler, A. Peeva, D. Pankin, A. Mücklich, R. A. Yankov, and W. Skorupa, Appl. Phys. Lett. **75**, 346 (1997).

11. A. A. Kalinin, V. M. Korol', N. A. Skakun, and S. K. Maksimov, in *Proceedings of the All-Union Workshop on Surface Diagnostics by Ion Beams* (Donetsk, 1980), p. 43.

12. L. C. Kimerling, P. J. Drevinsky, and C. S. Chen, in *Radiation Damage and Defects in Semiconductors* (Inst. Phys., London, 1973), p. 182.

13. J. Bacho, G. Kalinka, J. Keleti, et al., in *Ways to Improve Semiconductor Devices, Collection of Articles,* Preprint KIYaI-81-24 (Kiev. Inst. Yad. Issled., Kiev, 1981), p. 37.

14. *Physical Chemistry*, Vol. 2: *Electrochemistry, Chemical Kinetics and Catalysis*, Ed. by K. S. Krasnov (Vyssh. Shkola, Moscow, 2001), p. 119 [in Russian].

Translated by A. Spitsyn